Geophysical & Astrophysical Fluid Dynamics

The group velocity and radiation pattern of Rossby waves

J.F. McKenzie[a]

[a] School of Mathematics, Statistics and Physics, Durban University
of Technology, Durban, South Africa.
Published online: 06 May 2014.

PLEASE SCROLL DOWN FOR ARTICLE

Taylor & Francis
Taylor & Francis Group

The group velocity and radiation pattern of Rossby waves

J.F. MCKENZIE*

School of Mathematics, Statistics and Physics, Durban University of Technology,
Durban, South Africa

The propagation properties of mid-latitude Rossby waves are well known and are usually revealed in terms of the dispersion equation either in its diagnostic or wave normal forms, both of which show that phase propagation is entirely westward and is permitted only if the wave frequency is less than a certain critical frequency. Here we show that the group velocity diagram is an ellipse whose focus lies at the origin. This simple result supplements the Longuet-Higgins (1964) interpretation in which the wave normal curve is an offset circle, in elucidating the propagation properties of Rossby waves. In the case of a general β, which describes both topographic zonal variations as well as the latitudinal and spatial variations of the Coriolis effect, we show that these results hold through a rotation to a new set of coordinates. The stationary phase method shows that the radiation pattern generated by a time harmonic spatially compact source consists of two sets of hyperbolae exhibiting westward pointing "Mach-Froude" like lines, in a manner analogous to the generation of capillary-gravity waves by a moving object on the surface of deep water. These results are confirmed by the Green's function for the system which consists of a westward propagating wave superimposed on the Hankel function of zero order, appropriate to the 2-D Helmholtz equation.

Keywords: Group velocity; Radiation patterns for Rossby waves

1. Introduction

Rossby waves play a central role in geophysical fluid dynamics and dynamical meteorology, particularly in the dynamics of quasi-geostrophic flow. These waves arise from the latitudinal variation of the Coriolis force (through the Coriolis parameter f) and the near balance achieved between it and the pressure gradient, and are intimately connected with the conservation of potential vorticity (see, e.g. Vallis 2006). Their reflection properties at coast lines help to explain certain features of western boundary currents (Pedlosky 1987, Marshall and Plumb 2008). The anisotropic and dispersive propagation properties of Rossby waves (in particular the "backward" property in which phase and group velocities are opposite in the N-S direction) have been invoked, together with equatorial heating, to explain dipole-like formation of equatorial easterly jets accompanied, at higher latitudes, by westerly jets (Diamond *et al.* 2008). Also an inverse turbulent cascade together with Rossby waves can lead to the formation of zonal flows (Vallis 2006). These ideas have been further developed recently (Kidston and Vallis 2012) in models of an eddy-driven jet.

*Email: mckenziej@ukzn.ac.za

The properties of planetary waves in a rotating fluid using the β-plane approximation leading to the Rossby wave equation have been extensively discussed and the reader is referred to the texts of Gill (1982), Pedlosky (1987, 2003) and Vallis (2006) for a review of the subject. The use of Fourier analysis, the method of stationary phase, wave normal curves and their associated reciprocal polars, as methods for calculating the solution to linear wave problems and the corresponding radiation patterns are elucidated in Lighthills's work "Waves in Fluids" (Lighthill 1978).

In this paper, we apply these methods to "mid-latitude" Rossby waves for which the dispersion equation in both diagnostic and wave normal forms is well known. In particular, the wave normal in $\boldsymbol{k}$-space is an offset circle (Longuet-Higgins 1964) which shows that phase propagation is entirely westward. This diagram also shows that the ray direction, given by the normal to the curve, is directed eastward for short wavelengths and westward for long wavelengths. Expressions for the zonal and latitudinal group speeds are readily available but are usually left in a somewhat unperspicaceous form in which the zonal number k_x serves as a generating parameter for the group velocity diagram (e.g. Farrell and Watterson 1985, Lu and Boyd 2008). From a few simple algebraic steps which eliminates k_x in favour of the zonal group velocity, it follows that the group velocity is in fact an ellipse (Duba and McKenzie 2012), in which the focus is at the origin. This simple geometrical result supplements the Longuet-Higgins wave normal circle in revealing the properties of Rossby waves. It is also shown that in the more general case in which topographic, as well as Coriolis, β plane effects are present, the corresponding wave normal curves and group velocity diagrams are obtained by simple rotations through an angle measuring the ratio between the latitudinal and zonal β-effects.

Finally, using the method of stationary phase, we show that the radiation pattern generated by a time harmonic, spatially compact source, consists of two families of hyperbolae. The one completely surrounding the source corresponds to short wavelengths, permits a portion of eastward propagation, whereas the other is associated with longer wavelengths and lies completely to the west. Both patterns are asymptotic to a "Mach-Froude" like angle at which the short and long wavelengths wave numbers coalesce. These results are also revealed by the Green's function, for the time harmonic Rossby wave equation, which consists of the zero-order Hankel function with a superimposed westward propagating wave.

2. Rossby wave and dispersion equations

The linearized shallow water equations for a rotating layer of fluid of depth $H(x, y)$ lead, in the "low frequency", quasi-geostrophic approximation, to the classical Rossby wave equation for the displacement η of the surface (see the Appendix)

$$\frac{\partial}{\partial t}\left[\frac{f_o^2}{c_o^2} - \left(\frac{\partial^2}{\partial x^2} + \frac{\partial^2}{\partial y^2}\right)\right]\eta = -(\boldsymbol{\beta} \times \boldsymbol{\nabla}\eta)_z, \tag{1}$$

in which

$$\boldsymbol{\beta} = \boldsymbol{\beta}_t + \boldsymbol{\beta}_c, \qquad \boldsymbol{\beta}_t = -f\left(\frac{1}{c^2}\frac{\partial c^2}{\partial x}, \frac{1}{c^2}\frac{\partial c^2}{\partial y}\right), \qquad \boldsymbol{\beta}_c = \left(0, \frac{\partial f}{\partial y}\right), \tag{2a–c}$$

$$c_o = \sqrt{gH}, \qquad \text{shallow water speed}, \tag{2d}$$

$$f = f_0 + \beta_y y, \qquad \beta_{cy} = \frac{2\Omega\cos\theta_0}{R}, \qquad f_0 = 2\Omega\sin\theta_0. \tag{2e–g}$$

The suffix o denotes a reference level. We note here that the definition of $\boldsymbol{\beta}$ includes both the topographic β effect given by $\boldsymbol{\beta}_t$ and the Coriolis β effect $\boldsymbol{\beta}_c$. Equations (1) and (2) extend the analysis of Pedlosky (1987) to include the Coriolis as well as topographic β-effects. The scale analysis given in the appendix demonstrates that this extension is not entirely trivial. Here θ_0 is the latitude at which the β-plane is constructed tangent to the surface of the planet (radius R), rotating with angular frequency Ω, and y measures distance northward while x is directed eastward.

Equation (1) yields the well-known dispersion equation (Gill 1982, Pedlosky 1987, Pedlosky 2003) for plane waves varying as $\exp i(\omega t - k_x x - k_y y)$:

$$\omega = \frac{-\beta_y k_x + \beta_x k_y}{\left(k_x^2 + k_y^2 + f_o^2/c_o^2\right)}. \tag{3a}$$

This dispersion equation may also be written in form of wave number (or wave normal) curve,

$$\left(k_y - \frac{\beta_x}{2\omega}\right)^2 + \left(k_x + \frac{\beta_y}{2\omega}\right)^2 = \frac{\beta_x^2 + \beta_y^2}{4\omega^2} - \frac{f_o^2}{c_o^2}. \tag{3b}$$

Hence for a given angular frequency ω, the wave normal curve in wave number (k_x, k_y), space is circle-centred at $\left(\beta_x/2\omega, -\beta_y/2\omega\right)$ of radius given by the square root of the right-hand side of (3b), which requires the frequency ω to be less than the critical frequency $(c_o \beta/2 f_0)$, above which the wave is evanescent. If we write

$$\boldsymbol{\beta} = (\beta_x, \beta_y) = \beta(\cos\alpha, \sin\alpha), \tag{4}$$

it is clear that (3b) can be written as the Longuet-Higgins circle (Gill 1982) in the coordinates (k_y', k_x') obtained from (k_y, k_x) by rotating these clockwise through an angle α leading to equation (3) being replaced by

$$\omega = \frac{-\beta k_x'}{k_x'^2 + k_y'^2 + f_o^2/c_o^2}, \qquad k_y'^2 + \left(k_x' + \frac{\beta}{2\omega}\right)^2 = \left(\frac{\beta}{2\omega}\right)^2 - \frac{f_o^2}{c_o^2}. \tag{5a,b}$$

Figure 1 shows the wave normal circle rotated through an angle α.

In a recent paper (Duba and McKenzie 2012), it is shown that the phase (V_p) and group (V_g) velocity diagrams are, respectively, circles and ellipses displaced westward. In the present context of a general $\boldsymbol{\beta}$ (see (4)), the rotated phase velocity diagram becomes the circle

$$\bar{V}_{py}'^2 + \left(\bar{V}_{px}' + \frac{m}{2}\right)^2 = \frac{m^2}{4}\left(1 - \frac{4\bar{\omega}^2}{m}\right), \tag{6}$$

in which V_p' is normalized to c_o, $\bar{\omega} = \omega/\sqrt{\beta c_o}$ and the parameter m which is given by

$$m = \beta c_o / f_o^2, \tag{7}$$

is in fact the ratio of the Rossby speed (at long wavelengths, $k' \to 0$) to the shallow water speed. The dimensionless group velocity $\bar{V}_g'$ diagram, rotated clockwise through angle α, may be written

$$\frac{\bar{V}_{gy}'^2}{b^2} + \left[V_{gx}' + \frac{m}{2}\left(1 - \frac{4\bar{\omega}^2}{m}\right)\right]^2 \bigg/ a^2 = 1, \tag{8a}$$

in which the semi-major and minor axes of the ellipse are given by

$$a^2 = \frac{m^2}{4}\left(1 - \frac{4\bar{\omega}^2}{m}\right), \qquad b^2 = m\bar{\omega}^2\left(1 - \frac{4\bar{\omega}^2}{m}\right). \tag{8b,c}$$
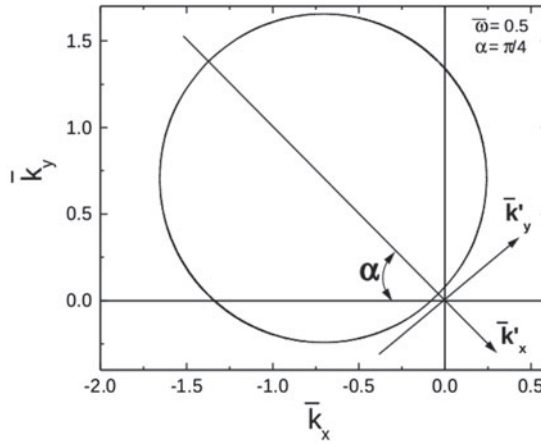
Figure 1. The wave normal curve is the Longuet-Higgins offset circle rotated through an angle α.

Equation (8) can be written in the polar form of an ellipse, namely

$$\bar{V}_g' = \frac{p}{1 + e\cos\chi}, \tag{9a}$$

in which

$$p = \frac{b^2}{a} = 2\bar{\omega}^2\left(1 - \frac{4\bar{\omega}^2}{m}\right)^{1/2}, \qquad e = \sqrt{1 - \frac{b^2}{a^2}} = \left(1 - \frac{4\bar{\omega}^2}{m}\right)^{1/2}. \tag{9b,c}$$

The shift along the negative V_{gx}' axis

$$\frac{m}{2}\left(1 - \frac{4\bar{\omega}^2}{m}\right) = \frac{ep}{1 - e^2}, \tag{10}$$

shows that the **origin** in the (V_{gy}', V_{gx}') $(= V_g'(\sin\chi, \cos\chi))$ plane is at the **focus** of the ellipse of eccentricity e. In terms of $\bar{\omega}$ and m, the ellipse (9a) may be written

$$V_g' = 2\bar{\omega}^2 \Big/ \left[\left(1 - \frac{4\bar{\omega}^2}{m}\right)^{-1/2} + \cos\chi\right]. \tag{11}$$

Note that in the limit $m \to \infty$, the V_g' curve becomes a parabola, as shown by the broken curve in figure 2.

These forms for the group velocity show that it scales like the square of the frequency divided by β for low frequencies, but as $\bar{\omega} \to \sqrt{m}/2$, $V_g' \to 0$, the ellipse collapses to the origin, with evanescence for $\bar{\omega} > \sqrt{m}/2$. At a fixed ω, the ellipse becomes more elongated as m increases, corresponding to the increase of the group velocity with Rossby radius in the manner of the radical $\sqrt{1 - 4\bar{\omega}^2/m}$. The maximum "eastward", "westward" and "northward" group speeds follow immediately from the major and minor axes as

$$V_{E,W} = \frac{m}{2}\left(1 - \frac{4\bar{\omega}^2}{m}\right)^{1/2}\left[\pm 1 - \left(1 - \frac{4\bar{\omega}^2}{m}\right)^{1/2}\right], \tag{12a}$$

$$V_{N(S)} = \bar{\omega}m^{1/2}\left(1 - \frac{4\bar{\omega}^2}{m}\right)^{1/2}. \tag{12b}$$
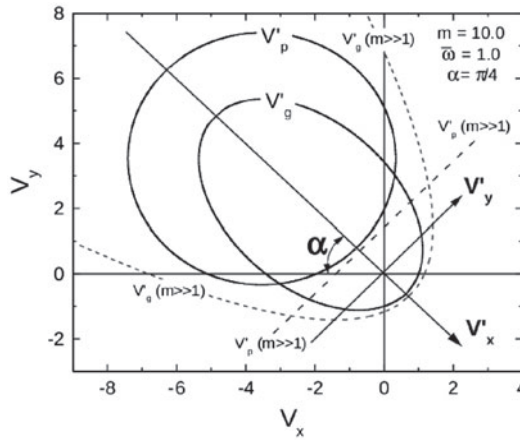
Figure 2. The phase V_p and group V_g velocity diagrams. In the limit $m \to \infty$, these tend to the line and parabola, respectively, as indicated by broken curves.
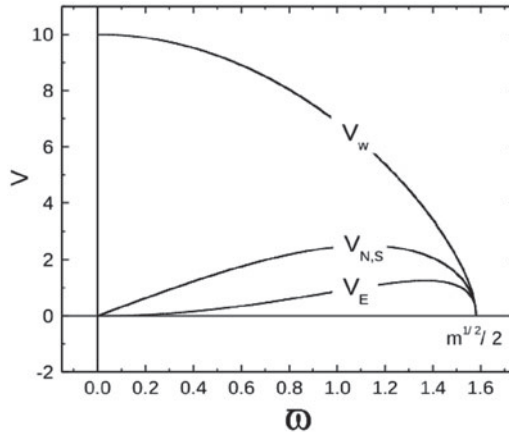
Figure 3. The maximum westward, eastward ($V_{W,E}$) and northward (southward) $V_{N,S}$ group speeds as a function of frequency.

These relations are depicted in figure 3. In summary, the group velocity diagram, namely an ellipse with the focus at the origin and the semi-major and minor axes functions of frequency and m, demonstrates in a clear fashion the highly dispersive and anisotropic nature of Rossby wave energy propagation.

3. Radiation pattern (stationary phase and Green's function)

The propagation properties of the Rossby group velocity outlined in the previous section are closely connected with and govern the radiation pattern generated by some given time harmonic, spatially compact source. In fact, it is the group velocity which determines the ray directions along which disturbances are propagated and constructively interfere to produce the dominant contribution to the far (radiation) field, along similar lines to the principles of "geometric optics" and Huyghens principle. The evolution of atmospheric waves generated

by point impulses has been analysed in a classic paper by Dickinson (1969). Here, we provide a brief discussion, restricted to Rossby waves on a β-plane, which makes use of the ideas of stationary phase to elucidate the radiation pattern excited by a given time harmonic, compact source. We show that the pattern consists of two families of hyperbolae, one corresponding to short wavelengths and the other to long wavelengths, both of which are asymptotic to a "Mach-Froude" type line making an angle χ_m with the west (but see below). This result supplements the original analysis of Dickinson (1969) and also later work by Rhines (2003).

We have seen, in the previous section 2, that in the case of a general $\boldsymbol{\beta}$, the classic Rossby wave and dispersion equations may be obtained by simple rotations in space (and/or wave number vector) through an angle measuring the ratio of the latitudinal to zonal β-effects. It is therefore sufficient to only consider the usual β effect since the case of a general $\boldsymbol{\beta}$ simply involves a rotation of axes. Hence, we consider the disturbance generated by a given time harmonic source, $\exp(i\omega t)S(x, y)$, can be calculated from the Rossby wave equation

$$\frac{\partial}{\partial t}\left[\left(\frac{\partial^2}{\partial x^2} + \frac{\partial^2}{\partial y^2}\right) - \kappa_o^2\right]\Psi + \beta\frac{\partial\Psi}{\partial x} = e^{i\omega t}S(x, y), \tag{13}$$

in which Ψ is a disturbance variable (such as the displacement η) and $S(x, y)$ is a given spatial distribution of the source, and $\kappa_o^2 = f_o^2/c_o^2$ is the square of the inverse Rossby radius. This wave equation also applies to a general β (i.e. topographic as well as Coriolis), as noted in section 2, by a rotation through an angle α to a new set of axes (x', y'), and therefore the solutions developed in this section also apply to the rotated system. This equation can be solved either using Fourier analysis or by standard Green's function approach. In the former method, if $s(k_x, k_y)$ is the 2-D Fourier transform of $S(x, y)$, then $\Psi(x, y)$ may be written as the Fourier synthesis of plane waves in the form,

$$\Psi = \frac{ie^{i\omega t}}{(2\pi)^2}\int_{-\infty}^{\infty}\int_{-\infty}^{\infty}\frac{s(k_x, k_y)e^{-i(k_x x + k_y y)}}{\left[\omega\left(k_y^2 + k_x^2 + \kappa_o^2\right) + \beta k_x\right]}\, dk_x\, dk_y. \tag{14}$$

The k_y integration is facilitated by the residue theorem using the fact that the integration has simple poles at

$$k_y = \pm\sqrt{\kappa_e^2 - \left(k_x + \frac{\beta}{2\omega}\right)^2}, \qquad \kappa_e^2 = \left(\frac{\beta}{2\omega}\right)^2 - \kappa_o^2. \tag{15a,b}$$

Equation (15a,b) is simply the dispersion equation for Rossby waves. The result for Ψ is

$$\Psi = -\frac{e^{i\omega t}}{4\pi\omega}\int_{-\infty}^{\infty}\frac{s(k_x, k_y)e^{-i(k_x x + k_y y)}}{2k_y}\, dk_x, \tag{16}$$

in which k_y is given by equation (15a,b). The sign in front of the radical for k_y is chosen according to the well-known property of Rossby waves, namely that the northward (southward) group velocity is in the opposite direction to the phase velocity ω/k_y. Hence, if we calculate the disturbance in the half space $y \gtrless 0$, we must choose $k_y \lessgtr 0$ to ensure that the energy propagates "away" from the source. In the case of a point source for which the Fourier transform $s(k_x, k_y)$ is simply a constant representing its strength, the integral in (16) can be shown to represent a westward zonal propagation combined with a zero Hankel function (but see the discussion below of the Green's function).

The main contribution to plane wave integrals of the form (16) comes from those points of the (k_y, k_x) wave normal curve for which the phase $\phi(x, y) = k_x x + k_y y$ is "stationary" for large values of (x, y), which corresponds to the radiation field. Thus, the phase is stationary (and the main disturbance Ψ results from constructive interference) at those points (x, y) for
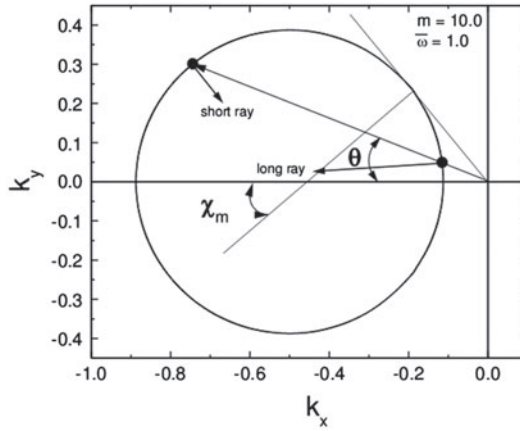
Figure 4. The radiation pattern of Rossby waves generated by a compact source around the origin. The "short" wavelengths completely surround the origin, whilst the "long" wavelengths lie entirely westward. Both families of hyperbolae are asymptotic to a "Mach-Froude" type cone making an χ_m with the west.

which

$$x + \frac{\partial k_y}{\partial k_x} y = 0, \tag{17a}$$

which is equivalent to the ratio y/x, as given by the ratio of the group velocities i.e.

$$\frac{y}{x} = \frac{\partial \omega/\partial k_y}{\partial \omega/\partial k_x} = -\frac{1}{\partial k_y/\partial k_x}, \tag{17b}$$

(see, e.g. Karoly and Hoskins 1982, Shaman *et al.* 2012, for a detailed discussion of developments in Rossby wave of ray tracing). In this last form, it is clear that the direction of the ray (group velocity) is parallel to the normal to the wave normal curve. The Rossby wave dispersion equation (the offset circle) gives stationary phase as occurring at

$$\frac{\partial k_y}{\partial k_x} = -\frac{\left[k_x + \beta/(2\omega)\right]}{k_y} = \frac{-\left[k_x + \beta/(2\omega)\right]}{\pm\sqrt{\kappa_e^2 - \left[k_x + \beta/(2\omega)\right]^2}} = -\frac{x}{y}. \tag{18}$$

Squaring (18) yields

$$\left(k_x + \frac{\beta}{2\omega}\right)^2 = \kappa_e^2 \frac{x^2}{r^2}, \qquad\qquad k_y^2 = \kappa_e^2 \frac{y^2}{r^2}, \tag{19a,b}$$

where $r^2 = x^2 + y^2$. Inserting these values for (k_y, k_x) into the phase

$$\phi = -(k_x x + k_y y) \tag{20a}$$

yields

$$\phi = \frac{\beta}{2\omega}\left[x + \sqrt{1 - \left(\frac{2\omega\kappa}{\beta}\right)^2} r\right]. \tag{20b}$$

Thus for a given value of the phase ϕ, the curve given by (20) provides the radiation pattern in a fashion similar to that of the classic ship wave, involving the Kelvin wedge angle. Equation (20b) may also be written in the polar (r, χ) form

Figure 5.   The wave normal curve showing that at a given wave normal angle θ there are two values of $\boldsymbol{k}$, corresponding to short and long wavelengths. The critical ray direction χ_m appears when the two values of k coalesce, and is parallel to the normal to the circle pointing along the radius in the direction χ_m.

$$\frac{\beta}{2\omega} r = \phi \Big/ \left[\sqrt{1 - \left(\frac{2\omega\kappa}{\beta}\right)^2} + \cos\chi \right]. \tag{21}$$

This represents two families of hyperbolae, one for $\phi > 0$ and the other for $\phi < 0$, both of which asymptote at the critical angle χ_m where

$$\cos\chi_m = -\sqrt{1 - \left(\frac{2\omega\kappa}{\beta}\right)^2}. \tag{22a}$$

These two families of radiation patterns are the long and short waves shown in figure 4. The family which completely surrounds the origin corresponds to the short wavelengths, whilst the family lying completely to the left of the origin is of long wavelength. The portions of the wave normal curve giving rise to each family are shown in figure 5. The critical angle χ_m, occurring where the two roots for $k(\theta)$ coalesce, is directed along the inward radius where $\boldsymbol{k}$ is tangential to the circle, showing that

$$\cos\chi_m = -\frac{\kappa_e}{\beta/(2\omega)}, \tag{22b}$$

at which $r \to \infty$ in accordance with (22a). This type of radiation pattern is similar to that of capillary-gravity waves generated by a moving source on deep water in which the capillary waves (short wavelengths) lie both ahead and entirely surround the object whilst the gravity waves (long wavelengths) lie completely behind (but see Doyle and McKenzie 2013, for a detailed discussion of this case). The existence of the asymptote at angle χ_m is a type of "Mach" type line which arises whenever the difference between the wave normal angle and the ray angle is 90 degrees (see e.g. Lighthill 1978, in which the stationary phase condition equation (17), yielding the radiation pattern, is interpreted as the reciprocal polar of the wave normal curve).

Finally, we note that these conditions also follow naturally from the Green's function of the wave equation (13), obtained by putting $S(x, y) = 4\pi\delta(x)\delta(y)$, and interpreting the k_x integral in (16) as a zero-order Hankel function combined with a superimposed westward wave shift.

Alternatively, we may seek a fundamental solution of equation (13) in the form

$$\Psi = \exp\left[i\left(\omega t + \frac{\beta}{2\omega}x\right)\right]R(r), \tag{23}$$

where $R(r)$ satisfies the Helmholtz equation namely,

$$\frac{1}{r}\frac{d}{dr}\left(r\frac{dR}{dr}\right) + \kappa_e^2 R = 0, \tag{24}$$

in which κ_e^2 is the square of the wave number given by (15b). This is the Bessel equation of zero order and argument $(\kappa_e r)$. Hence, the Green's function, which has a logarithmic singularity at the origin (the source point) and yields outgoing waves at infinity, is the zero-order Hankel equation (Morse and Feshbach 1953), combined with the superimposed westward phase propagation, that is to say,

$$\Psi = \frac{1}{\omega}\exp\left[i\left(\omega t + \frac{\beta}{2\omega}x\right)\right]H_0^{(1)}(\kappa_e r). \tag{25}$$

Observe that the superimposed westward phase propagation takes place at the phase speed $\omega^2/2\beta$ which is the zonal speed associated with the centre of the Longuet-Higgins circle. The asymptotic form of $H_0^{(1)}(\kappa_e r)$ as $r \to \infty$, immediately shows that the phase, which gives the radiation pattern, is

$$\frac{\beta}{2\omega}x + \kappa_e r = \text{const}. \tag{26}$$

This is in agreement with the arguments from stationary phase which lead to equation (21) for the two families of hyperbolae. We note that this also generalizes Rhines' result on the Green's function to allow for finite Rossby radius c/f_0 through the wave number given by (15b). The latter inclusion gives rise to the two families of hyperbolae rather than the single family of parabolas, which reflects the fact that in the limit $m \to \infty$ the group velocity tends to a parabola.

4. Summary

This paper elucidates certain propagation properties of Rossby waves. The first is that the group velocity diagram at a given frequency is an ellipse, whose focus coincides with the origin. This property stands alongside the Longuet-Higgins (1964) wave normal diagram which is a circle whose centre is displaced "westward". The second interesting property is the radiation pattern of Rossby waves generated by a time harmonic, spatially compact source. The method of stationary phase shows that this pattern consists of two families of hyperbolae, the one corresponding to short wavelengths completely surrounds the source (in a fashion similar to capillary waves which lie both ahead and behind an object in a stream), whereas the long wavelength one lies entirely westward; both sets of waves being asymptotic at a "Mach" type angle. This property is also revealed by the Green's function which is a combination of the zero-order Hankel function with superimposed westward propagation. These results supplement the work of Dickinson (1969) on the excitation of atmospheric waves by point sources.

References

Diamond, P.H., Gurcan, D.D., Hahn, T.S., Miki, K. and Garbet, X., Momentum theorems and the structure of atmospheric jets and zonal flows in plasmas. *Plasma Phys. Control. Fusion* 2008, **50**, 124018. doi:10.1088/0741-3335/50/12/124018.

Dickinson, R.E., Propagators of atmospheric motions. 1. Excitation by point impulses. *Rev. Geophys.* 1969, **7**, 483–514.

Doyle, T.B. and McKenzie, J.F., Stationary wave patterns in deep water. *Quaestiones Math.* 2013, **36**(4), 487–500.

Duba, C.T. and McKenzie, J.F., Propagation properties of Rossby waves for latitudinal β-plane variations of f and zonal variations of the shallow water speed. *Ann. Geophysicae.* 2012, **30**, 849–855.

Farrell, B. and Watterson, I., Rossby waves in opposing currents. *J. Atmos. Sci.* 1985, **42**, 1741–1756.

Gill, A.E., *Atmosphere and Ocean Dynamics*, p. 682, 1982 (Academic Press: London).

Karoly, D.J. and Hoskins, B.J., Three dimensional propagation of planetary waves. *J. Met. Soc. Japan* 1982, **60**, 109–123.

Kidston, J. and Vallis, G.K., The relationship between the speed and the latitude of an eddy-driven jet in a stirred barotropic model. *J. Atmos. Sci.* 2012, **69**, 3251–3263.

Lighthill, J., *Waves in Fluids*, p. 504, 1978 (Cambridge University Press: London).

Longuet-Higgins, M.S., On group velocity and energy flux in planetary wave motions. *Deep-Sea Res. Oceanogr. Abstracts* 1964, **11**, 35–42.

Lu, E. and Boyd, J.P., Rossby wave ray traveling in a barotropic divergent atmosphere. *J. Atmos. Sci.* 2008, **65**, 1679–1691.

Marshall, J., Plumb, R.A., *Atmosphere, Ocean, and Climate Dynamics (An Introductory Text)*, p. 319, 2008 (Academic Press (Elsevier): Waltham, MA).

Morse, P.M. and Feshbach, H., *Methods of Theoretical Physics*, Vol. 1, p. 997, 1953 (McGraw Hill: New York).

Pedlosky, J., *Geophysical Fluid Dynamics*, p. 710, 1987 (Springer-Verlag: New York).

Pedlosky, J., *Waves in the Ocean and Atmosphere (Introduction to Wave Dynamics)*, p. 403, 2003 (Springer-Verlag: New York).

Rhines, P.B., Rossby waves. In *Encyclopedia of Atmospheric Sciences*, edited by J.R. Holton, 2003 (Academic Press: Oxford).

Shaman, J., Samelson, R.M. and Tziperman, E., Complex wavenumber Rossby wave tracing. *J. Atmos. Sci.* 2012, **69**, 2112–2133.

Vallis, G.K., *Atmospheric Oceanic Fluid Dynamics, Fundamentals and Large-scale Circulation*, p. 745, 2006 (Cambridge University Press: Cambridge).

Appendix A: Rossby wave equation for topographic and Coriolis contributions to the β effect

The linearized shallow wave equations for the mass flux vector $\boldsymbol{Q} = H\boldsymbol{u}$ ($\boldsymbol{u}$ is the horizontal velocity) and the surface elevation η may be written (e.g. Pedlosky 1987, Duba and McKenzie 2012)

$$\frac{\partial Q_x}{\partial t} - f Q_y = -c^2 \frac{\partial \eta}{\partial x}, \tag{A.1}$$

$$\frac{\partial Q_y}{\partial t} + f Q_x = -c^2 \frac{\partial \eta}{\partial y}, \tag{A.2}$$

$$\frac{\partial \eta}{\partial t} + \left(\frac{\partial Q_x}{\partial x} + \frac{\partial Q_y}{\partial y} \right) = 0, \tag{A.3}$$

in which $c = \sqrt{gH}$ is the shallow water speed, $H(x, y)$ is the depth and $f(y)$ is the Coriolis parameter (frequency).

Operating on the first two equations yields

$$\left(\frac{\partial^2}{\partial t^2} + f^2 \right) Q_x = -c^2 \left(\frac{\partial^2 \eta}{\partial t \partial x} + f \frac{\partial \eta}{\partial y} \right), \tag{A.4}$$

$$\left(\frac{\partial^2}{\partial t^2} + f^2 \right) Q_y = -c^2 \left(\frac{\partial^2 \eta}{\partial t \partial y} - f \frac{\partial \eta}{\partial x} \right). \tag{A.5}$$

Do ∂(A.4)$/\partial x + \partial$(A.5)$/\partial y$, use (A.3) and rearrange to obtain

$$\frac{\partial}{\partial t}\left[\left(\frac{\partial^2}{\partial t^2} + f^2\right)\eta - \nabla\cdot(c^2\nabla\eta)\right] = \left(\nabla(fc^2) \times \nabla\eta\right)_z + 2ff'Q_y. \tag{A.6}$$

A similar equation for Q_y may be obtained by taking $\partial/\partial x$ of the curl of equations (A.1) and (A.2), to complete the system of coupled equations. However, we wish only to describe Rossby waves which are characterized by low frequencies ($\partial/\partial t \ll f$) and whose motions are in quasi-geostrophic balance. In such a case, we may neglect $\partial^2/\partial t^2$ compared with f^2 on the left-hand side of (A.6); Q_y may be approximated with its geostrophic value, namely

$$Q_y \approx \frac{c^2}{f}\frac{\partial\eta}{\partial x}, \tag{A.7}$$

and f and c are replaced with their reference values (f_o and c_o) except where their derivatives are taken to give the Coriolis and topographic β-effects. The wave equation (A.6) then simplifies to the classic Rossby wave equation (1) of the text, but with a generalized β.

This low frequency, quasi-geostrophic result can be justified in the following manner. The small parameter $\varepsilon = \omega/f$ and the dimensionless variables,

$$\boldsymbol{x} = (c_o/f_o)\bar{\boldsymbol{x}}, \qquad t = \bar{t}/\omega, \qquad \eta = H_o\bar{\eta}, \qquad Q_y = H_oc_0\bar{Q}_y, \qquad \text{(A.8a–d)}$$

together with the reference shallow water speed $c_o = \sqrt{gH_o}$ and Rossby radius c_o/f_o, where the overbar indicates dimensionless variables are introduced. We further assume that the variations in $\bar{H}$ and $\bar{f}$ are also of O(ε), that is

$$\bar{H} = 1 + \varepsilon\bar{h}(\bar{x}), \qquad\qquad \bar{f} = 1 + \varepsilon\bar{\beta}_c\bar{y}. \tag{A.9a,b}$$

With this ansatz, (A.6) takes the form

$$\varepsilon\frac{\partial}{\partial t}\left[\left(\varepsilon^2\frac{\partial^2}{\partial t^2} + (1 + \varepsilon\bar{\beta}_cy)^2\right)\bar{\eta} - (1 + \varepsilon\bar{h})\bar{\nabla}^2\bar{\eta} - \varepsilon\bar{\nabla}\bar{h}\cdot\bar{\nabla}\bar{\eta}\right]$$
$$= \varepsilon(1 + \varepsilon\bar{\beta}_cy)\left(\bar{\nabla}\bar{h} \times \bar{\nabla}\bar{\eta}\right)_z - \varepsilon(1 + \varepsilon\bar{h})\bar{\beta}_c\frac{\partial\bar{\eta}}{\partial\bar{x}} + 2\varepsilon^2\frac{\partial\bar{Q}_x}{\partial t}\bar{\beta}_{cy}. \tag{A.10}$$

Dividing through by the small parameter ε gives,

$$\frac{\partial}{\partial t}\left(\bar{\eta} - \bar{\nabla}^2\bar{\eta}\right) = \left((\bar{\nabla}\bar{h} - \bar{\boldsymbol{\beta}}_c) \times \bar{\nabla}\bar{\eta}\right)_z + \text{O}(\varepsilon). \tag{A.11}$$

Restoring the dimensions to (A.11) leads to the Rossby wave equation (1) in the text.